Supporting Information

Measurement report: Evaluation of sources and mixing state of black carbon aerosol under the background of emission reduction in the North China Plain: implications for radiative effect

Qiyuan Wang[1,2], Li Li[1], Jiamao Zhou[1], Jianhuai Ye[3], Wenting Dai[1], Huikun Liu[1], Yong Zhang[1], Renjian Zhang[4,5], Jie Tian[1], Yang Chen[6], Yunfei Wu[4], Weikang Ran[1], and Junji Cao[1,2]

[1]Key Laboratory of Aerosol Chemistry and Physics, State Key Laboratory of Loess and Quaternary Geology, Institute of Earth Environment, Chinese Academy of Sciences, Xi'an 710061, China
[2]CAS Center for Excellence in Quaternary Science and Global Change, Xi'an 710061, China
[3]School of Engineering and Applied Sciences, Harvard University, Cambridge, MA 02138, USA
[4]Key Laboratory of Regional Climate-Environment Research for Temperate East Asia, Institute of Atmospheric Physics, Chinese Academy of Sciences, Beijing 100029, China
[5]Xianghe Observatory of Whole Atmosphere, Institute of Atmospheric Physics, Chinese Academy of Sciences, Xianghe County, Hebei Province, 065400, China
[6]Chongqing Institute of Green and Intelligent Technology, Chinese Academy of Sciences, Chongqing 400714, China

Correspondence to: Qiyuan Wang (wangqy@ieecas.cn) and Junji Cao (cao@loess.llqg.ac.cn)

Contents of this file

Texts S1 to S2

Tables S1 to S3

Figures S1 to S6

Text S1. Configuration of Weather Research and Forecasting model coupled with chemistry (WRF-Chem)

The model resolution was 3 km × 3 km, and there were 300 grids in each of the latitude and longitude. The domain was concentrated in the North China Plain and the north of Hebei Province, with the central location at 39.00°N, 117.00°E. There were thirty-five vertical layers from the Earth's surface up to 50 hPa. The horizontal grid projection is Lambert. The meteorological fields were retrieved from the National Centers for Environmental Prediction (NCEP) reanalysis data, with a spatial and temporal resolution of 1° × 1° and 6 h, respectively (http://rda.ucar.edu/datasets/ds083.2). The initial and lateral BC boundary conditions were retrieved by the 6 h output of the Model for Ozone and Related chemical Tracers, version 4 (MOZART-4, Emmons et al., 2010). More detailed descriptions of configurations in WRF-Chem model in this study are summarized in Table S3. The BC emission inventory with a spatial resolution of 0.25° × 0.25° includes industry, power, transportation, and residential sources (e.g., fossil fuel and biofuel), which were based on the Multi-resolution Emission Inventory for China (MEIC) for the year of 2012 (www.meicmodel.org).

Text S2. Complementary data

Hourly wind speed (WS) was measured with an automatic weather station installed at the Xianghe Atmospheric Observatory. Hourly planetary boundary layer (PBL) heights were retrieved from the Hybrid Single-Particle Lagrangian Integrated Trajectory (HYSPLIT) model (Draxler and Rolph, 2003).

Table S1. Summary of the mass concentrations of black carbon (BC) and its contribution from different sources in China and other countries.

Region	Site type	Site	Period	[a]Method	[b]BC_{lff} (%)	[c]BC_{sf} (%)	[d]BC_{ff} (%)	[e]BC_{bb} (%)	Reference
China	Urban	Beijing	winter, 2015	aeth. mode	30	70			Liu et al., 2018
		Beijing	winter, 2013	$^{\Delta}$14C	8	92			Andersson et al., 2015
		Shanghai	winter, 2013	$^{\Delta}$14C	46	54			Andersson et al., 2015
		Guangzhou	winter, 2013	$^{\Delta}$14C	58	42			Andersson et al., 2015
	Suburban	Xianghe	winter, 2017	aeth. mode	69	31			This study
		Nanjing	winter, 2016	aeth. mode	84	16			Jing et al., 2019
Europe	Urban	Grenoble, France	winter	aeth. mode			82	18	Favez et al., 2010
		Paris, France	winter	aeth. mode			76	24	Crippa et al., 2013
		Madrid, Spain	winter	aeth. mode			93	7	Becerril-Valle et al., 2017
		Madrid, Spain	winter	aeth. mode			84	16	Becerril-Valle et al., 2017
		London, UK	winter	aeth. mode			77	23	Fuller et al., 2014
		Zurich, Switzerland	winter	aeth. mode			76	24	Herich et al., 2011
	Suburban	Paris, France	winter	aeth. mode			80	20	Crippa et al., 2013
		London, UK	winter	aeth. mode			85	15	Crilley et al., 2015
		Demokritos, Greece	winter	aeth. mode			67	33	Kalogridis et al., 2018
		Thiseio, Greece	winter	aeth. mode			71	29	Kalogridis et al., 2018
	Rural	Detling, Kent, England	winter	aeth. mode			70	30	Crilley et al., 2015

		Andalusia, Spain	winter	aeth. mode	12	88	Becerril-Valle et al., 2017
		Magadino-Cadenazzo, Swiss	winter	aeth. mode	70	30	Herich et al., 2011
		Payerne, Switzerland	winter	aeth. mode	67	33	Herich et al., 2011
		Swiss	winter	aeth. mode	49	51	Sandradewi et al., 2008
		Vavihill, Sweden	winter	aeth. mode	44	56	Martinsson et al., 2017
South Asia	Urban	Delhi, India	winter	aeth. mode	72	28	Dumka et al., 2018
		Ahmedadbad, India	winter	aeth. mode	77	23	Rajesh and Ramachandran, 2017
		Gorakhpur, India	winter	aeth. mode	74	26	Vaishya et al., 2017
		IITM-Pashan, India	winter	aeth. mode	85	15	Kolhe et al., 2019

[a]aeth. mode represents aethalometer model.

[b-e]BC_{lff}, BC_{sf}, BC_{ff}, and BC_{bb} describe BC from liquid fossil fuel source, solid fuel source, fossil fuel source, and biomass burning, respectively.

Table S2. Descriptions of six different black carbon (BC) source regions in the case study for the Weather Research and Forecasting model coupled with chemistry (WRF-Chem).

Source Region	Location(s) of BC sources
Region 1	Xianghe
Region 2	Beijing
Region 3	Tianjin
Region 4	North China Plain (including south Hebei Province, northwest Shandong Province
Region 5	North Hebei Province
Region 6	Other areas that not included in Region 1 – 5

Table S3. Summary of the configurations of Weather Research and Forecasting model coupled with chemistry (WRF-Chem).

Configuration	Description
Region	The North China Plain and north of Hebei Province
Simulation period	2-14 January 2018
Domain size	300 × 300
Domain center	39.00°N, 117.00°E
Horizontal resolution	3 km × 3 km
Vertical resolution	Thirty-five vertical layers from the Earth's surface up to 50 hPa
Microphysics scheme	WSM 5-classes microphysics scheme (Hong and Lim, 2006)
Boundary layer scheme	YSU PBL scheme (Hong et al., 2006)
Surface layer scheme	MM5 similarity (Zhang and Anthes, 1982)
Land-surface scheme	Noah land-surface model (Chen and Dudhia, 2001)
Longwave radiation scheme	RRTM scheme (Mlawer et al., 1997)
Shortwave radiation scheme	MM5 shortwave scheme (Dudhia, 1989)
Meteorological boundary and initial conditions	NCEP 1° × 1° reanalysis data
Chemical boundary and initial conditions	MOZART 6-h output (Emmons et al., 2010)
Anthropogenic emission inventory	industry, power, transportation, and residential sources (e.g., fossil fuel and biofuel)

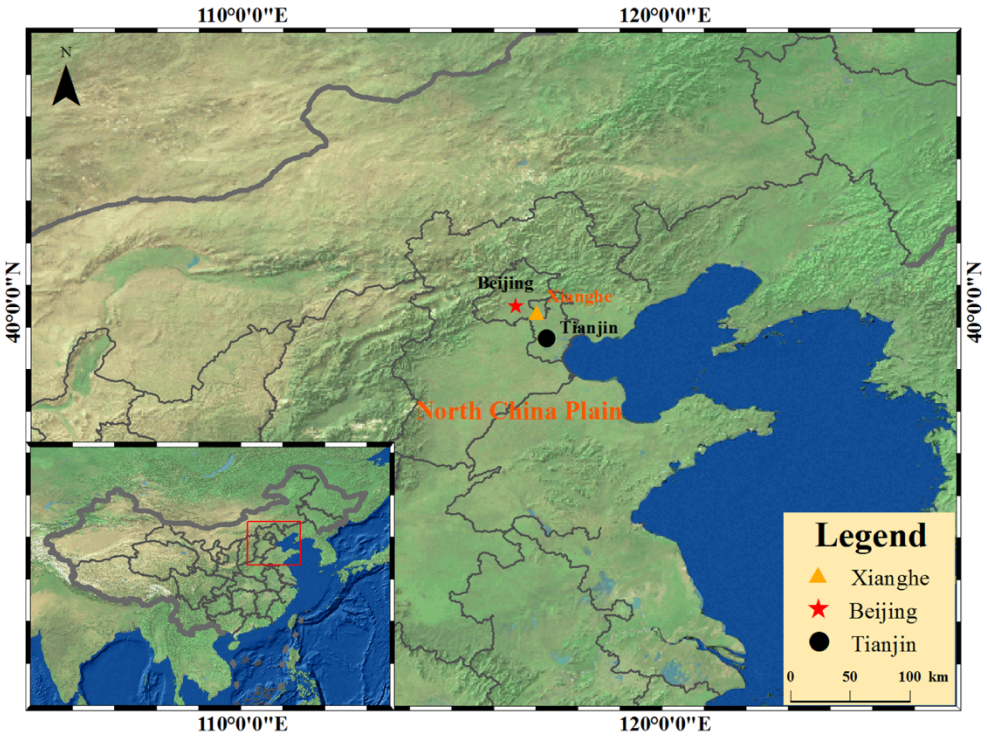

Figure S1. Map showing the Xianghe sampling site and surrounding areas. The map was drawn using ArcGIS software. The base map is the World Topographic Map from © ESRI (Environmental Systems Research Institute, Inc.) (www.arcgis.com/home/item.html?id=30e5fe3149c34df1ba922e6f5bbf808f).

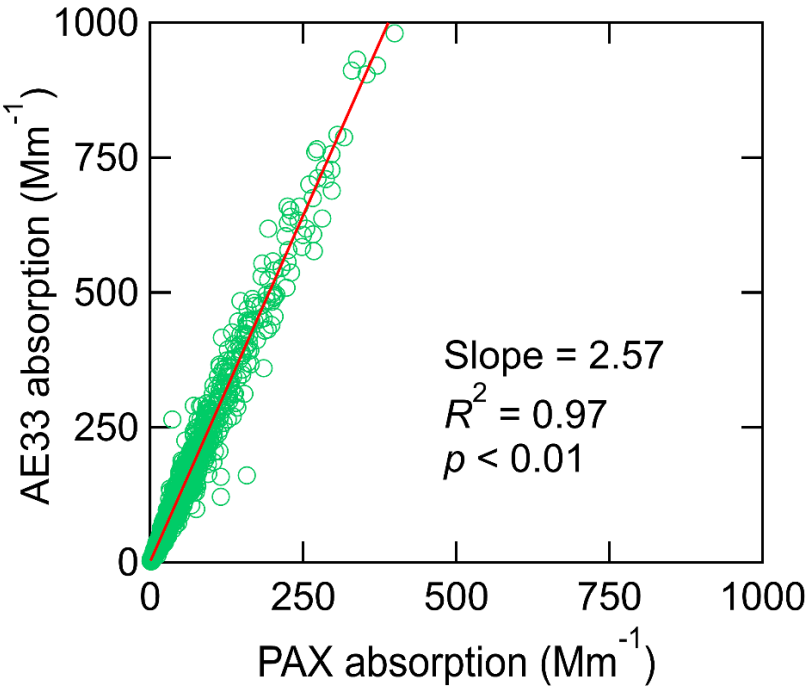

Figure S2. Relationship between the light absorption coefficient measured by multi-wavelength aethalometer (Model AE33) at wavelength of 520 nm and photoacoustic extinctiometer (PAX) at wavelength of 532 nm.

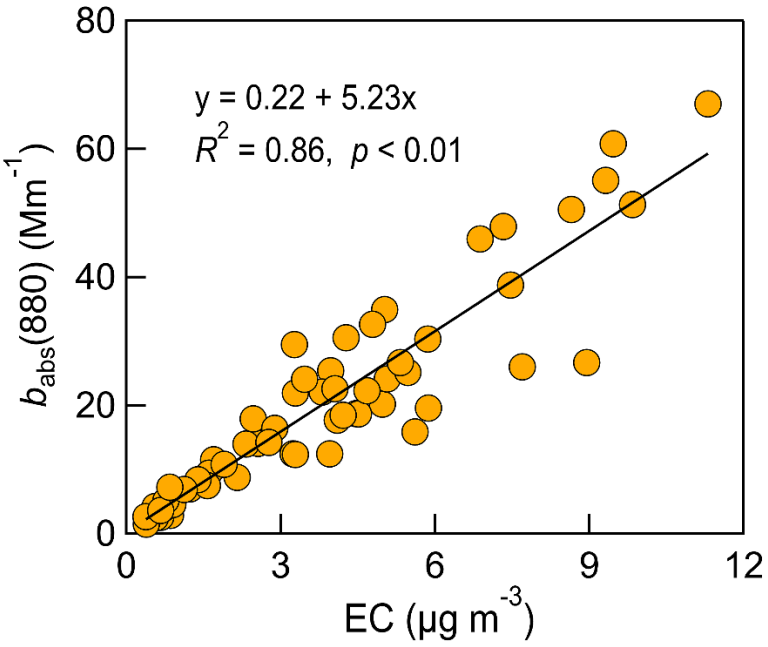

Figure S3. Relationship between the light absorption measured by multi-wavelength aethalometer at wavelength of 880 nm (b_{abs}(880)) and the mass concentration of elemental carbon (EC).

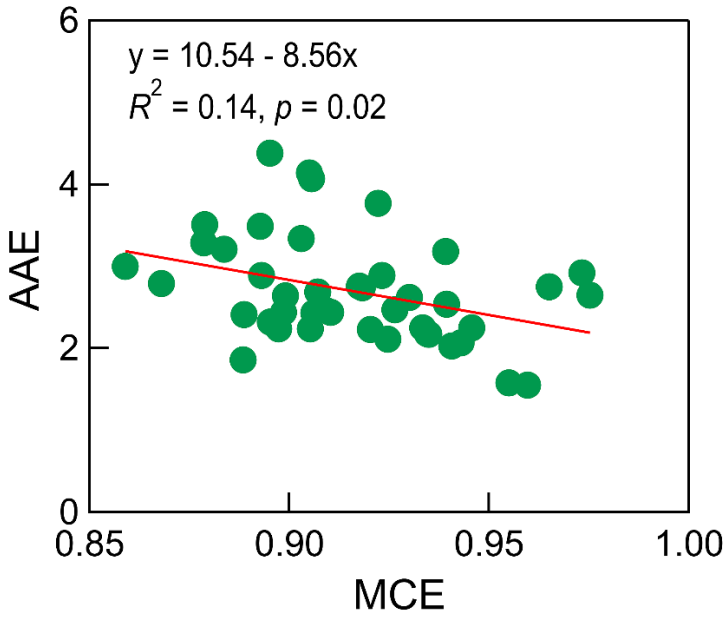

Figure S4. Relationship between the aerosol absorption Ångström exponent (AAE) in solid fuel emissions and the corresponding modified combustion efficiency (MCE). The MCE was calculated with carbon dioxide and carbon monoxide.

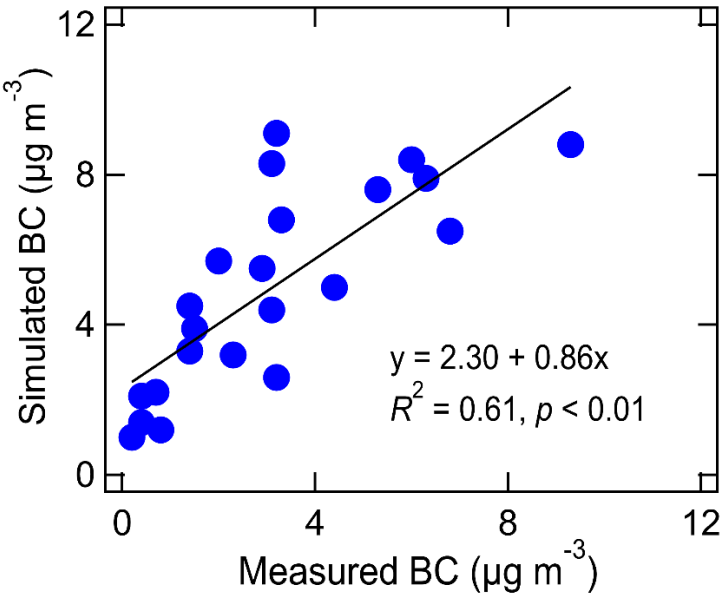

Figure S5. Relationship between the simulated black carbon (BC) with the Weather Research and Forecasting model coupled with chemistry (WRF-Chem) and the measured BC.

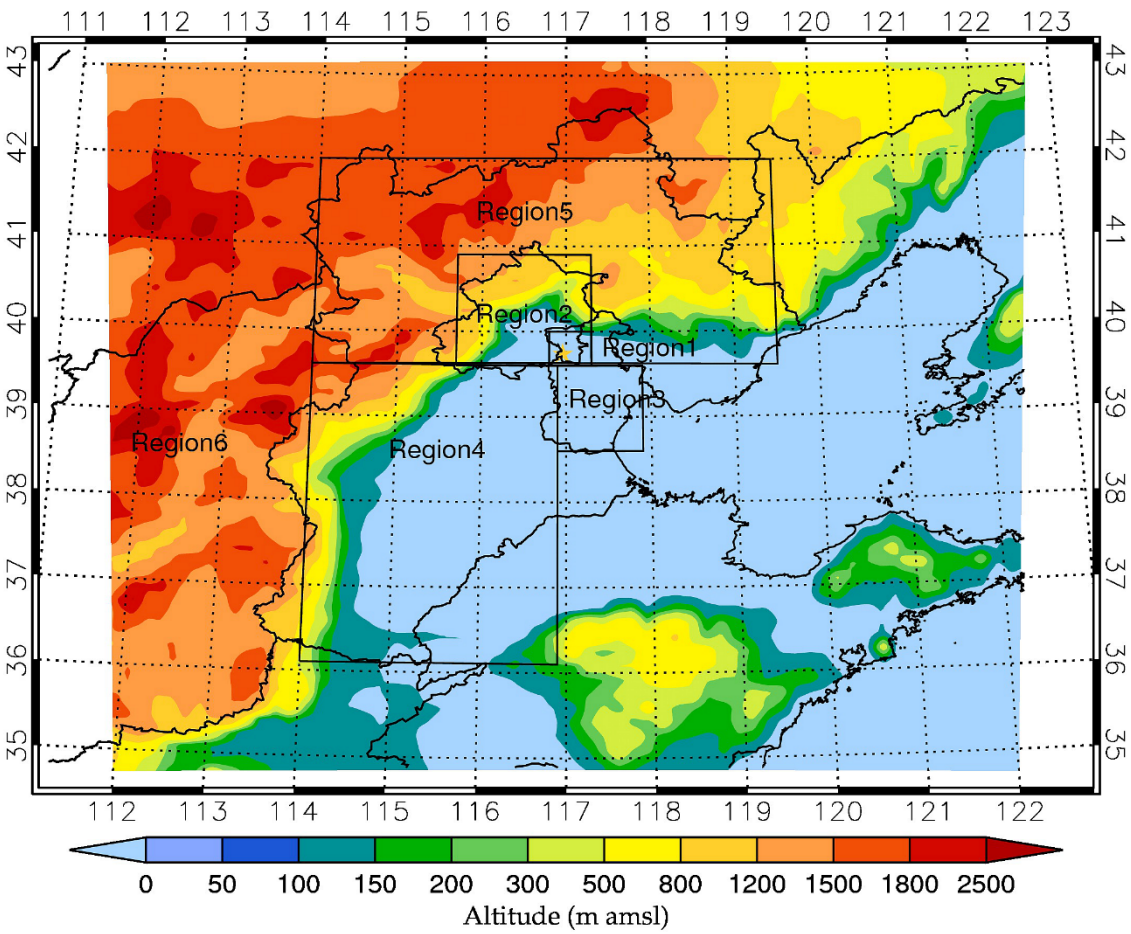

Figure S6. Division of different regions in the Weather Research and Forecasting model coupled with chemistry (WRF-Chem).

References:

Andersson, A., J. Deng, K. Du, M. Zheng, C. Yan, M. Sköld, & Ö. Gustafsson (2015). Regionally-varying combustion sources of the January 2013 severe haze events over eastern China. *Environmental Science & Technology*, 49(4), 2038–2043. https://doi.org/10.1021/es503855e

Becerril-Valle, M., Coz, E., Prévôt, A. S. H., Močnik, G., Pandis, S. N., Sánchez de la Campa, A. M., et al. (2017). Characterization of atmospheric black carbon and co-pollutants in urban and rural areas of Spain. *Atmospheric Environment*, 169, 36–53. https://doi.org/10.1016/j.atmosenv.2017.09.014

Chen, F., & Dudhia, J. (2001). Coupling an advanced land surface-hydrology model with the Penn State-NCAR MM5 modeling system. Part I: Model implementation and sensitivity. *Monthly Weather Review*, 129, 569–585. https://doi.org/10.1175/1520-0493(2001)129<0569:Caalsh>2.0.Co;2

Crilley, L. R., Bloss, W. J., Yin, J., Beddows, D. C. S., Harrison, R. M., Allan, J. D., et al. (2015), Sources and contributions of wood smoke during winter in London: assessing local and regional influences. *Atmospheric Chemistry and Physics*, 15(6), 3149–3171. https://doi.org/10.5194/acp-15-3149-2015

Crippa, M., DeCarlo, P. F., Slowik, J. G., Mohr, C., Heringa, M. F., Chirico, R., et al. (2013). Wintertime aerosol chemical composition and source apportionment of the organic fraction in the metropolitan area of Paris. *Atmospheric Chemistry and Physics*, 13(2), 961–981. https://doi.org/10.5194/acp-13-961-2013

Draxler, R. R., and Rolph, G. D.: HYSPLIT (HYbrid Single-Particle Lagrangian Integrated Trajectory), Silver Spring, MD, Model access via NOAA ARL READY Website, available at: https://ready.arl.noaa.gov/HYSPLIT.php (last access: August 2019), 2003.

Dudhia, J. (1989). Numerical study of convection observed during the winter monsoon experiment using a mesoscale two-dimensional model. *Journal of the Atmospheric Sciences*, 46, 3077–3107. https://doi.org/10.1175/1520-0469(1989)046<3077:Nsocod>2.0.Co;2

Dumka, U. C., Kaskaoutis, D. G., Tiwari, S. Safai, P. D., Attri, S. D., Soni, V. K., et al. (2018). Assessment of biomass burning and fossil fuel contribution to black carbon

concentrations in Delhi during winter. *Atmospheric Environment*, 194, 93–109. https://doi.org/10.1016/j.atmosenv.2018.09.033

Emmons, L. K., Walters, S., Hess, P. G., Lamarque, J. F., Pfister, G. G., Fillmore, D., et al., (2010). Description and evaluation of the Model for Ozone and Related chemical Tracers, version 4 (MOZART-4). *Geoscientific Model Development*, 3, 43–67. https://doi.org/10.5194/gmd-3-43-2010, 2010

Favez, O., EI Haddad, I., Piot, C., Boréave, A., Abidi, E., Marchand, N., et al. (2010). Inter-comparison of source apportionment models for the estimation of wood burning aerosols during wintertime in an Alpine city (Grenoble, France). *Atmospheric Chemistry and Physics*, 10(12), 5295–5314. https://doi.org/doi:10.5194/acp-10-5295-2010

Fuller, G. W., Tremper, A. H., Baker, T. D., Yttri, K. E., & Butterfield, D. (2014). Contribution of wood burning to PM_{10} in London. *Atmospheric Environment*, 87, 87–94. https://doi.org/10.1016/j.atmosenv.2013.12.037

Herich, H., Hueglin, C., & Buchmann, B. (2011). A 2.5 year's source apportionment study of black carbon from wood burning and fossil fuel combustion at urban and rural sites in Switzerland. *Atmospheric Measurement Techniques*, 4(7), 1409-1420. https://doi.org/10.5194/amt-4-1409-2011

Hong, S.-Y., & Lim, J.-O. J. (2006). The WRF single-moment 6-class microphysics scheme (WSM6). *Journal of the Korean Meteorological Society*, 42, 129–151.

Hong, S.-Y., Noh, Y., & Dudhia, J. (2006). A new vertical diffusion package with an explicit treatment of entrainment processes. *Monthly Weather Review*, 134, 2318–2341. https://doi.org/10.1175/mwr3199.1

Jing, A., Zhu, B., Wang, H., Yu, X., An, J., & Kang H. (2019). Source apportionment of black carbon in different seasons in the northern suburb of Nanjing, China. *Atmospheric Environment*, 201, 190–200. https://doi.org/10.1016/j.atmosenv.2018.12.060

Kalogridis, A. C., Vratolis, S., Liakakou, E., Gerasopoulos, E., Mihalopoulos, N., & Eleftheriadis, K. (2018). Assessment of wood burning versus fossil fuel contribution to wintertime black carbon and carbon monoxide concentrations in Athens, Greece.

Atmospheric Chemistry and Physics, 18(14), 10219–10236. https://doi.org/10.5194/acp-18-10219-2018

Kolhe, A. R., Ralegankar, S. D., Safai, P. D., & Aher, G. R. (2019). Absorption properties of black carbon aerosols over environmentally distinct locations in south-western India: Temporal, spectral characterization and source apportionment. *Journal of Atmospheric and Solar-Terrestrial Physics*, 189, 1–17. https://doi.org/10.1016/j.jastp.2019.03.010

Liu, Y., Yan, C., & Zheng, M. (2018). Source apportionment of black carbon during winter in Beijing. *Science of The Total Environment*, 618, 531–541. https://doi.org/10.1016/j.scitotenv.2017.11.053

Martinsson, J., Abdul Azeem, H., Sporre, M. K., Bergström, R., Ahlberg, E., Öström, E., et al., A. (2017). Carbonaceous aerosol source apportionment using the Aethalometer model – evaluation by radiocarbon and levoglucosan analysis at a rural background site in southern Sweden. *Atmospheric Chemistry and Physics*, 17(6), 4265–4281. https://doi.org/10.5194/acp-17-4265-2017

Mlawer, E. J., Taubman, S. J., Brown, P. D., Iacono, M. J., & Clough, S. A. (1997). Radiative transfer for inhomogeneous atmospheres: RRTM, a validated correlated-k model for the longwave. *Journal of Geophysical Research-Atmospheres*, 102, 16663–16682. https://doi.org/10.1029/97jd00237

Rajesh, T. A., & Ramachandran, S. (2017). Characteristics and source apportionment of black carbon aerosols over an urban site. *Environmental Science and Pollution Research*, 24(9), 8411–8424. https://doi.org/10.1007/s11356-017-8453-3

Sandradewi, J., Prévôt, A. S. H., Szidat, S., Perron, N., Alfarra, M. R., Lanz, V. A., et al. (2008). Using aerosol light absorption measurements for the quantitative determination of wood burning and traffic emission contributions to particulate matter. *Environmental Science & Technology*, 42(9), 3316–3323. https://doi.org/10.1021/es702253m

Vaishya, A., Singh, P., Rastogi, S., & Babu, S. S. (2017). Aerosol black carbon quantification in the central Indo-Gangetic Plain: Seasonal heterogeneity and source apportionment. *Atmospheric Research*, 185, 13-21. https://doi.org/10.1016/j.atmosres.2016.10.001

Zhang, D., & Anthes, R. A. (1982). A high-resolution model of the planetary boundary-layer –sensitivity tests and comparisons with sesame-79 data. *Journal of Applied Meteorology*, 21, 1594–1609, https://doi.org/10.1175/1520-0450(1982)021<1594:Ahrmot>2.0.Co;2